Ion drag force in plasmas at high electronegativity

I. Denysenko,[1,*] M. Y. Yu,[1] L. Stenflo,[2] and S. Xu[3]
[1]*Theoretical Physics I, Ruhr University, D-44780 Bochum, Germany*
[2]*Department of Physics, Umeå University, SE-90187 Umeå, Sweden*
[3]*Plasma Sources and Applications Center, NIE, School of Physical and Mathematical Sciences, Nanyang Technological University, 1 Nanyang Walk, 637616 Singapore*
(Received 31 March 2005; published 28 July 2005)

The electric as well as the positive- and negative-ion drag forces on an isolated dust grain in an electronegative plasma are studied for large negative-ion densities, when the negative ions are not Boltzmann distributed. The investigation is carried out for submicrometer dust particles, so that the theory of Coulomb scattering is applicable for describing ion-dust interaction. Among the forces acting on the dust grain, the negative-ion drag force is found to be important. The effects of the negative-ion density, neutral-gas pressure, and dust-grain size on the forces are also considered. It is shown that by increasing the density of the negative ions one can effectively manipulate the dust grains. Our results imply that both dust voids and balls can be formed.

DOI: 10.1103/PhysRevE.72.016405 PACS number(s): 52.25.Vy, 52.27.Lw, 52.77.Dq, 52.80.Pi

I. INTRODUCTION

There is much recent interest in complex (dusty) plasmas because plasma-produced nano- and microparticles are indispensable in many modern applications [1], such as in the fabrication of composite materials, silicon films, ultrahard coatings, etc. They are also of basic physical interest because many fundamental processes (phase transitions, transport, wave propagation, clustering, etc.) in these macroscopic systems are similar to that at the atomic level [2–8].

Recently, experiments have demonstrated the existence of novel self-organized structures such as dust voids [9,10] and dust balls [6,8]. Such structures clearly depend on the distribution of the various forces acting on the dust particles. Depending on the plasma conditions, forces such as gravity, electric, positive ion, electron and neutral drag, as well as thermophoresis, can play important roles [11–13]. A detailed knowledge of these forces is thus important for understanding and controlling the transport of the grains, the equilibrium states, as well as the wave phenomena in complex plasma systems.

Most of the existing studies of dusty plasmas are devoted to electropositive plasmas where only positively charged ions are present, although electronegative plasmas are widely used in plasma technologies [14] and dust growth is often observed in such discharges [1,4]. Only recently has there been increased attention to dusty plasmas containing negative ions. Among others, problems of linear wave propagation, diffusion of plasma particles, equilibrium states, and sheath structure in dusty electronegative plasmas have been considered [15–19]. In particular, the ion drag forces on a dust grain in an electronegative complex plasma with Boltzmann negative ions were also recently investigated [20]. It was found that in general the positive-ion drag force is larger than that of the negative ions, and that the number of locations where the ion drag forces balance the electric force is considerably larger than that in an electropositive plasma.

However, because of the many physical processes existing in a typical dusty discharge, the assumption of Boltzmann density for the negative ions holds only when the ion loss is predominantly due to ion diffusion to the walls [14]. At relatively large ($\geqslant 10^{10}$ cm^{-3}) ion densities typical for modern plasma sources [14] or pressures ($\geqslant$100 mTorr) typical for many dusty plasma experiments [1], ion-ion recombination becomes important and the Boltzmann density for the negative ions is no longer valid.

The present paper focuses on the positive- and negative-ion drag forces arising from momentum transfer from the ions drifting relative to an isolated charged grain at high negative-ion densities (high electronegativity [14]). We found that the negative- and positive-ion drag forces can become similar in magnitude. This occurs when the negative- and positive-ion fluxes are nearly the same. The effects of negative-ion concentration, neutral-gas pressure, and dust size on the force balance are also investigated. It is shown that by varying the parameters of the discharge one can control the forces and, as a result, also the location and motion of an isolated dust grain. In particular, one can conclude that both dust voids and balls can appear, depending on how the force balance on a grain occurs.

II. THEORETICAL MODEL

A. Fluid model of the plasma

Consider a steady-state plasma containing singly charged positive and negative ions, electrons, as well as neutral particles. All the species interact among themselves as well as with each other. The plasma is located in a cylindrical discharge chamber of large aspect ratio ($L \ll D$, where L and D are the height and diameter of the plasma, respectively), so that all the plasma parameters depend only on the coordinate x perpendicular to the planes bounding the plasma slab. For

*Corresponding author. Permanent address: School of Physics and Technology, Kharkiv National University, 61077 Kharkiv, Ukraine. Email address: deny@tp1.rub.de

 ©2005 The American Physical Society

simplicity, it is assumed that the electron temperature T_e is spatially constant. Therefore, the plasma is symmetrical with respect to the center of the slab ($x=0$). It is assumed that there is an isolated dust grain in the plasma. We shall consider the forces acting on the grain for different grain locations. The effect of the dust grain on the electron and ion densities as well as the electron temperature is negligible.

We also assume that the neutral gas pressure is sufficiently high such that the condition $\lambda_+ T_e/LT_+ \leqslant 1$ is satisfied. Here, λ_+ is the positive-ion mean free path and T_+ is the positive-ion temperature. The positive- and negative-ion fluxes are then [14]

$$\Gamma_\alpha = -D_\alpha \partial_x n_\alpha \pm n_\alpha \mu_\alpha E, \tag{1}$$

where $\alpha=+$ and $-$ denote the positive and negative ions, E is the electric field, and n_α, D_α, and μ_α are the density, diffusion coefficient, and mobility coefficient, respectively. The mobility coefficient μ_α (in $m^2/V\,s$) is calculated using the low-E-field Langevin mobility expression [21]

$$\mu_\alpha = 0.514 \frac{T_{gas}}{p\sqrt{\alpha_\alpha m_r}},$$

where the reduced mass m_r is in amu, the polarizability of the gas molecule α_α is in $Å^3$, p is the gas pressure in pascals, and T_{gas} is the gas temperature in kelvins. D_α is obtained from the well-known Einstein relation $D_\alpha = k_B T_\alpha \mu_\alpha / e$ between the diffusion and mobility coefficients. It is also assumed that the positive- and negative-ion diffusion and mobility coefficients are equal.

Furthermore, it is assumed that the plasma is quasineutral, or

$$n_+ = n_- + n_e, \tag{2}$$

where n_e is the electron density. The electrons obey the Boltzmann density profile

$$n_e = n_{e0} \exp(e\Phi/k_B T_e), \tag{3}$$

where n_{e0} is the electron density at the center of the plasma slab, k_B is the Boltzmann constant, e is the magnitude of the electron charge, and Φ is the plasma potential, giving the electric field $E=-\partial_x \Phi$.

The continuity equations for the positive and negative ions are [14]

$$d_x \Gamma_+ = K_{iz} n_0 n_e - K_{rec} n_- n_+ \tag{4}$$

and

$$d_x \Gamma_- = K_{att} n_0 n_e - K_{rec} n_- n_+, \tag{5}$$

where n_0 is the neutral gas density, and K_{iz}, K_{rec}, and K_{att} are the ionization, recombination, and attachment rate constants, respectively.

At the discharge center ($x=0$), symmetry requires that the electron and ion density gradients be zero. The densities in the discharge center are taken to be known parameters. We shall consider relatively high plasma densities when the sheath size is smaller than the slab size. Therefore, the positive-ion velocity at the plasma boundary $x=L/2$ is given by the Bohm velocity [14]

$$u_B = \sqrt{\frac{k_B T_e (n_e + n_-)}{M_+ (n_e + n_- T_e/T_-)}}, \tag{6}$$

which reduces to the familiar Bohm expression $u_{B0} = \sqrt{k_B T_e / M_+}$ when $n_-=0$. Note that $u_B < u_{B0}$ for $n_- T_e / T_- n_e > 1$. The electron temperature T_e can depend on the slab size. Without loss in generality, in the calculations we shall vary T_e for fixed plasma size.

For convenience, the governing physical quantities are normalized as follows: $\tilde{n}_\alpha = n_\alpha / n_{e0}$, $\tilde{\Gamma}_\alpha = \Gamma_\alpha / n_{e0} c_s$, and $\xi = x/\Lambda$. The ion acoustic speed c_s in the absence of negative ions is given by $c_s = \sqrt{k_B T_e / M_+}$, where M_+ is the mass of the positive ions, and the ionization length is $\Lambda = c_s / K_{iz} n_0$. From Eqs. (1), (4), and (5), taking into account Eqs. (2) and (3), we obtain after normalization

$$d_\xi \tilde{\Gamma}_+ = \tilde{n}_e - \beta_{rec} \tilde{n}_+ (\tilde{n}_+ - \tilde{n}_e),$$

$$d_\xi \tilde{\Gamma}_- = \beta_{att} \tilde{n}_e - \beta_{rec} \tilde{n}_+ (\tilde{n}_+ - \tilde{n}_e),$$

$$\tilde{\Gamma}_+ = -\tilde{D}_+ d_\xi \tilde{n}_+ - \epsilon \tilde{\mu}_+,$$

$$\tilde{\Gamma}_- = -\tilde{D}_- d_\xi (\tilde{n}_+ - \tilde{n}_e) + \epsilon \tilde{\mu}_- - \tilde{\mu}_- d_\xi \tilde{n}_e,$$

$$\epsilon = (\tilde{n}_+ / \tilde{n}_e) d_\xi \tilde{n}_e, \tag{7}$$

where $\beta_{rec} = K_{rec} n_{e0} / K_{iz} n_0$, $\beta_{att} = K_{att} n_{e0} / K_{iz} n_0$, $\tilde{\mu}_\alpha = k_B T_e \mu_\alpha / e c_s \Lambda$, and $\tilde{D}_\alpha = D_\alpha / c_s \Lambda$.

The equations (7) are integrated using a first-order implicit method [20,22]. For more details about the method, we refer to Ref. [20] and (15.6.24) of Ref. [22].

B. Ion drag forces

In a low-temperature discharge a dust grain experiences several forces. Here we shall concentrate on the positive- and negative-ion drag and electric forces, which are the most important under the conditions given. The electric force acting on an isolated dust grain in the plasma is given by $\mathbf{F}_e = eZ_d \mathbf{E}$, where Z_d is the dust charge. The positive- and negative-ion drag forces can be obtained by assuming that the ion distribution functions are given by drifting Maxwellians [1], or

$$f_\alpha = \left(\frac{M_\alpha}{2\pi k_B T_\alpha} \right)^{3/2} \exp\left(- \frac{M_\alpha [v_y^2 + v_z^2 + (v_x - u_\alpha)^2]}{2 k_B T_\alpha} \right), \tag{8}$$

where M_α is the mass of the positive and negative ions, and v_x, v_y, and v_z are the velocity components. The positive- and negative-ion drift velocities $u_+(x)$ and $u_-(x)$ in the field E are $u_+(x) = \Gamma_+(x)/n_+(x)$ and $u_-(x) = \Gamma_-(x)/n_-(x)$, respectively.

The drag force on an isolated dust grain can been represented by a sum of the "collection" and "orbital" forces [1]. The positive- and negative-ion drag forces are [1]

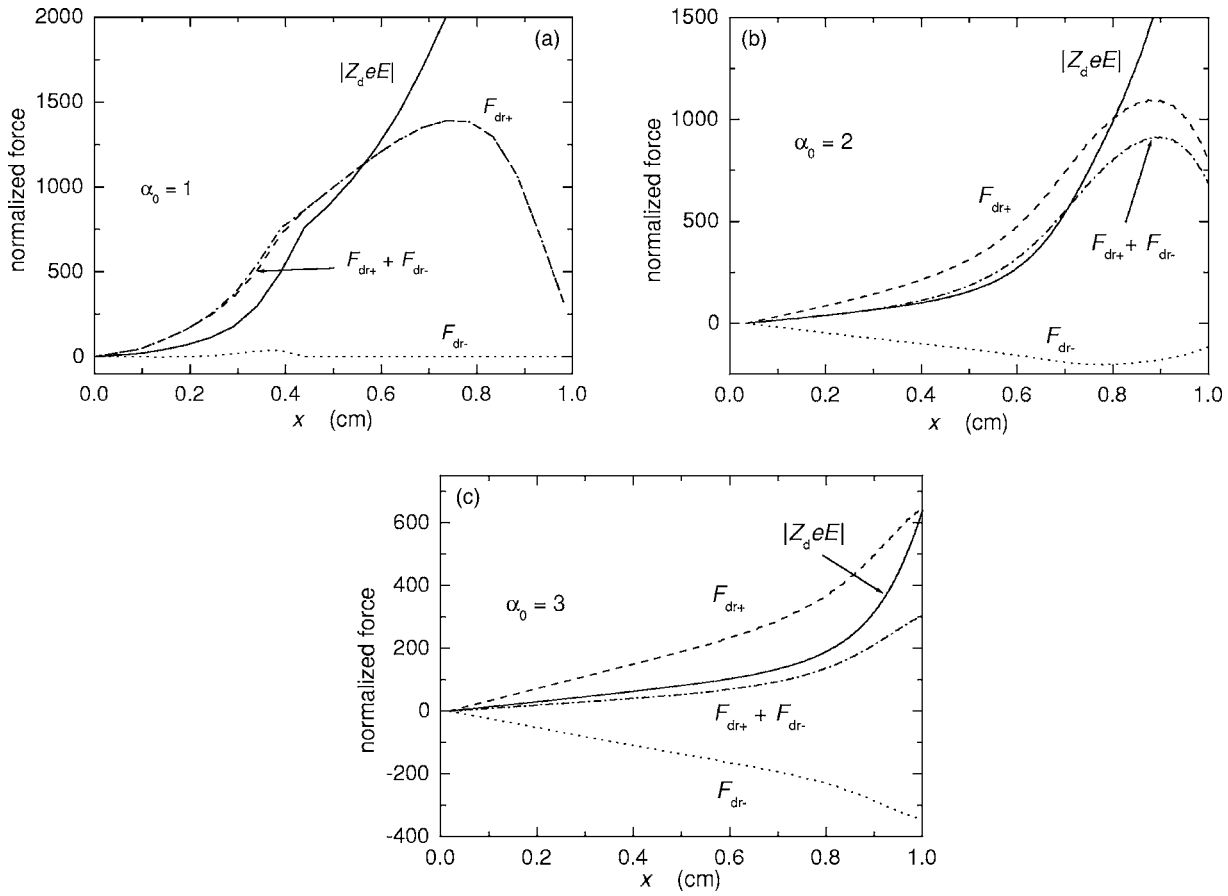

FIG. 1. The normalized forces for $\alpha_0=1$ (a), 2 (b), and 3 (c). The forces are calculated for $p_0=200$ mTorr, $n_{e0}=10^{10}$ cm^{-3}, $T_+=500$ K, $a_d=50$ nm, and normalized by $k_B T_e/\Lambda$. Here, $x=0$ and 1 cm are the center and boundary of the plasma slab of height $L=2.0$ cm.

$$\mathbf{F}_{dr\alpha}^{c,o} = n_\alpha M_\alpha \int_{-\infty}^{+\infty} \sigma_\alpha^{c,o}(v) v \mathbf{v} f_\alpha(\mathbf{v}) d^3\mathbf{v}, \tag{9}$$

where $\sigma_\alpha^{c,o}$ is the momentum-transfer cross section for ion collection, and the orbital momentum-transfer cross section, respectively.

The x component of the force is therefore [13,23]

$$F_{dr\alpha}^{c,o} = \frac{2n_\alpha M_\alpha}{u_\alpha v_{0\alpha}\sqrt{\pi}} \int_0^\infty \sigma_\alpha^{c,o}(v) v^3 \exp\left(-\frac{v^2+u_\alpha^2}{v_{0\alpha}^2}\right)\left[\cosh\left(\frac{2u_\alpha v}{v_{0\alpha}^2}\right) - \frac{v_{0\alpha}^2}{2u_\alpha v}\sinh\left(\frac{2u_\alpha v}{v_{0\alpha}^2}\right)\right] dv, \tag{10}$$

where $v_{0\alpha}=\sqrt{2k_B T_\alpha/M_\alpha}$.

The momentum-transfer cross section for ion collection is [1]

$$\sigma_\alpha^c(v) = \pi b_{coll}^2,$$

where $b_{coll}=a_d(1\pm 2b_{\pi/2}/a_d)^{1/2}$, a_d is the dust radius, and $b_{\pi/2}=e^2|Z_d|/M_\alpha v^2$. For negative ions $b_{coll}=0$ for $b_{\pi/2}>a_d/2$.

The orbital momentum-transfer cross section can be expressed as [1,13]

$$\sigma_\alpha^o(v) = 2\pi b_{\pi/2}^2 \ln\left(\frac{\lambda_D^2 + b_{\pi/2}^2}{b_{coll}^2 + b_{\pi/2}^2}\right), \tag{11}$$

where λ_D is the Debye length. For the electronegative plasma the Debye length is [24]

$$\lambda_D = [4\pi e^2(n_e/k_B T_e + n_-/k_B T_- + n_+/2E_+)]^{-0.5},$$

where $E_+=m_+\bar{u}_+^2/2$, and $\bar{u}_+=\sqrt{u_+^2+8k_B T_+/M_+\pi}$.

The negative-ion orbital and collection cross sections are similar to the cross sections for electron-dust collisions [25]. In order to make use of the cross sections in our calculations, we need to find the dust-grain charge.

The dust charge is found by balancing the plasma currents on the dust grain

$$I_+ = I_e + I_-,$$

where I_α is the local current of particle α onto the dust grain. The ion current is given by $I_+=\pi a_d^2 e n_+ \bar{u}_+(1+2e^2|Z_d|/a_d M_+ \bar{u}_+^2)$. The electron and negative-ion grain currents are approximately given by

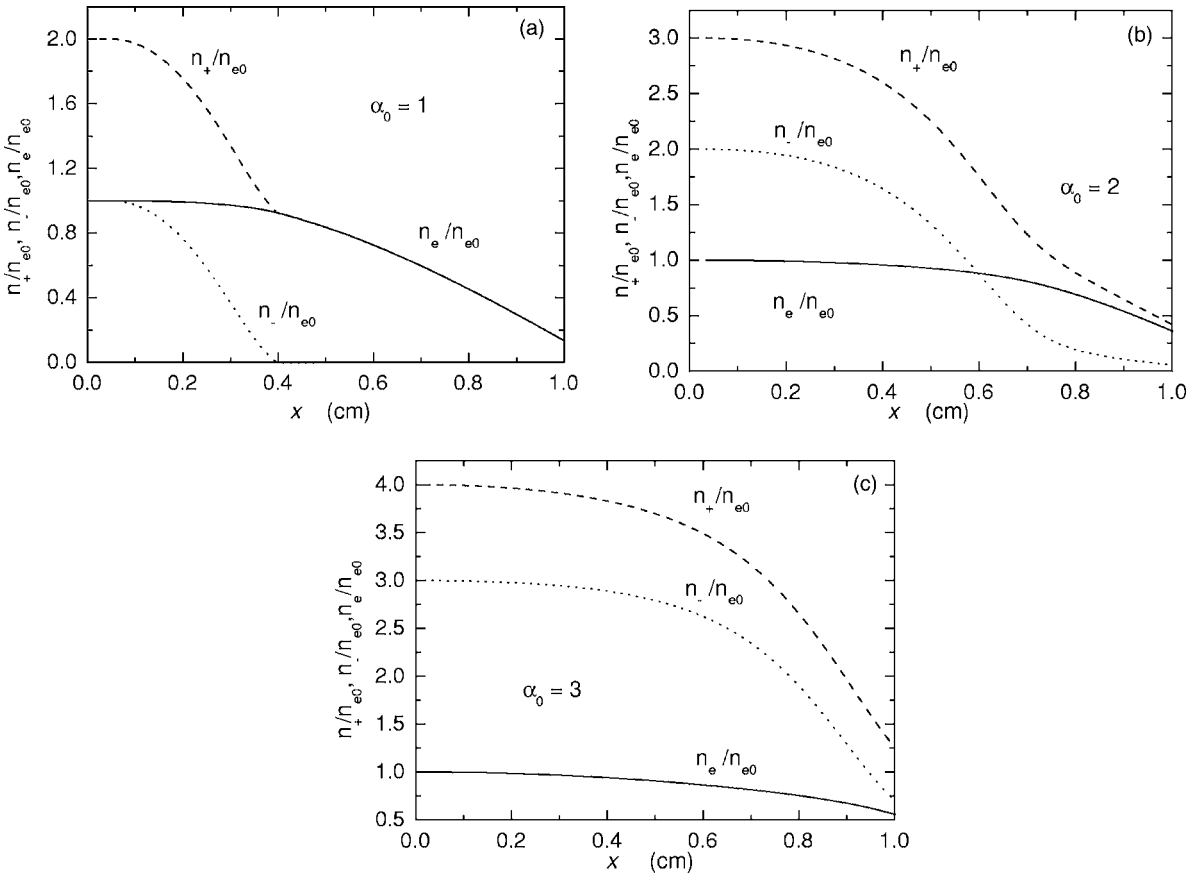

FIG. 2. The effect of increasing the negative-ion density on the spatial profiles of the electrons and the positive and negative ions. The profiles are for $\alpha_0=1$ (a), 2 (b), and 3 (c). The other plasma parameters are the same as in Fig. 1.

$$I_{e,-} = \pi a_d^2 e n_{e,-} \sqrt{\frac{8k_B T_{e,-}}{\pi M_{e,-}}} \exp\left(\frac{-e^2|Z_d|}{a_d k_B T_{e,-}}\right),$$

where we have $T_e \gg T_-$ for the parameters considered. For consistency we shall set $T_-=T_+$. That is, the electron current on a dust grain is much higher than that of the negative ions. However, the negative-ion current can substantially affect the dust charging if the negative-ion speed is sufficiently high [26].

We shall apply the present model to a silane plasma, assuming that SiH_3^+ and SiH_3^- are the dominant ions in the plasma [27]. The expressions for the collision rates can be found elsewhere [16].

For comparison, the traditional expression for the positive-ion drag force is [1]

$$F_{dr+}^{approx} = n_+ M_+ v_+ [\sigma_+^o(v_+) + \sigma_+^c(v_+)] u_+, \tag{12}$$

where $v_+ = \sqrt{u_+^2 + 8k_B T_+/\pi M_+}$. Similarly, the corresponding negative-ion force is

$$F_{dr-}^{approx} = n_- M_- v_- [\sigma_-^o(v_-) + \sigma_-^c(v_-)] u_-, \tag{13}$$

where $v_- = \sqrt{u_-^2 + 8k_B T_-/\pi M_-}$.

In the next section we shall show that the negative-ion drag force calculated from the simplified expression (13) is of about the same magnitude as that from Eq. (10). The term $n_- M_- v_- \sigma_-^c u_-$ can be excluded from Eq. (13) because most of the negative ions in the distribution (8) do not arrive at the negatively charged dust.

III. RESULTS

First we consider the effect of the negative-ion density on the other plasma parameters as well as the drag and electric forces on the dust grain. The profiles of the forces for different $\alpha_0 = n_-(0)/n_e(0)$ are shown in Fig. 1. The electron, positive-, and negative-ion density profiles under the same conditions are given in Fig. 2. One can see that with increase of n_- the negative-ion drag force also increases with respect to the positive-ion drag and electric forces. The increase can be attributed to an enhancement of the negative-ion flux which at relatively large n_- is directed toward the center of the discharge. From Eq. (5) one then obtains

$$\Gamma_-(x) = \int_0^x K_{att} n_0 n_e dx - \int_0^x K_{rec} n_+ n_- dx, \tag{14}$$

from which (and also Fig. 3) one can see that $\Gamma_-(x)$ is positive for small n_- and n_+, i.e., the flux is directed away from the center of the discharge. On the other hand, we have $\Gamma_-(x) < 0$ for large n_-. In this case the negative ions move to the discharge center, pushing the dust grains in the same direction. At small α_0 the negative-ion flux is significantly

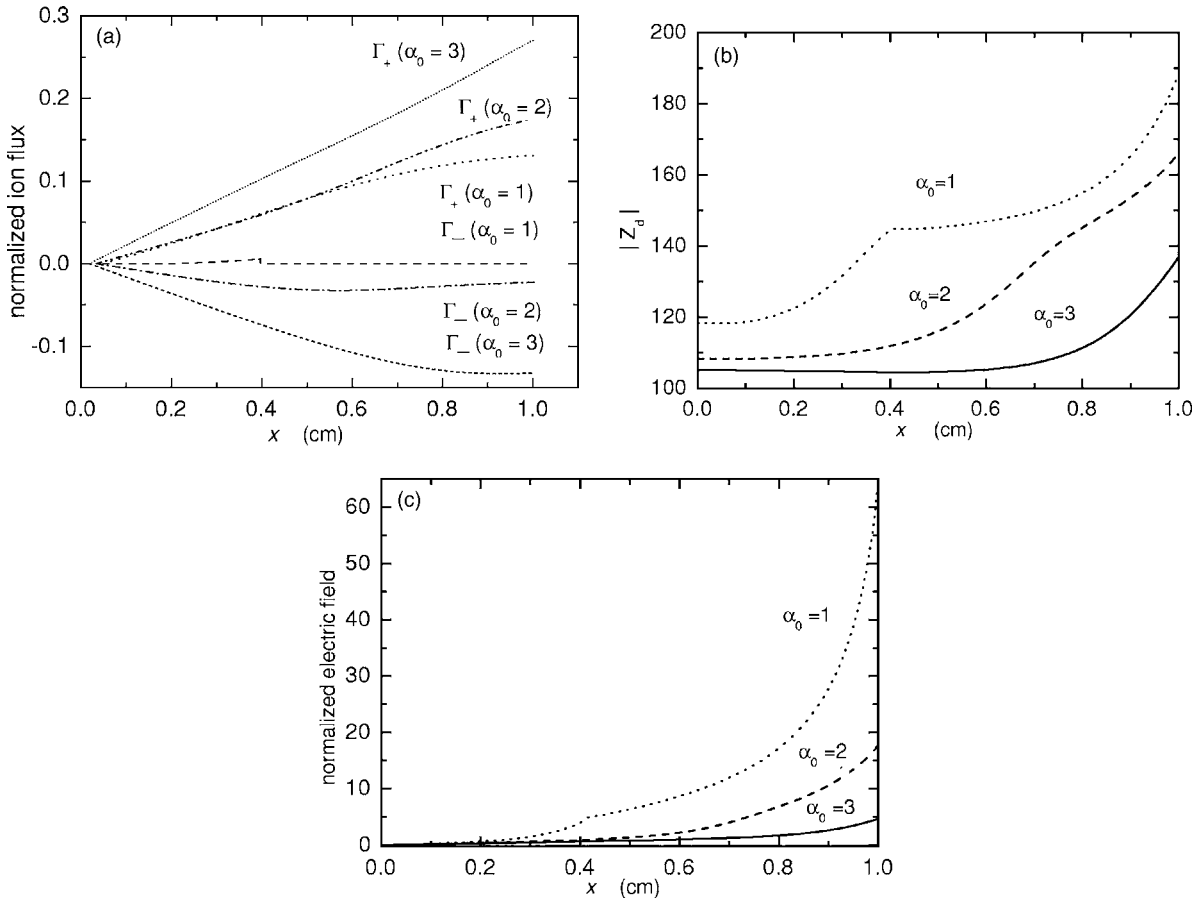

FIG. 3. (a) The positive- and negative-ion fluxes, (b) the dust charge, and (c) the normalized electric field for different negative-ion densities. The other plasma parameters are the same as in Fig. 1.

smaller than that of the positive ions, as shown in Fig. 3(a). At large α_0, the positive- and negative-ion fluxes have almost the same magnitude. As a result the total ion drag force $F_{dr+}+F_{dr-}$ decreases significantly as compared to F_{dr+} alone (see Fig. 1). One can also see that at small α_0 the total drag force is larger than the electric force $|Z_d eE|$ at $x<0.5$ cm. At large α_0, due to increase of $|F_{dr-}|$ the total ion drag force is smaller than $|Z_d eE|$ throughout the plasma slab.

In Figs. 3(b) and 3(c), the dust charge and normalized electric field $eE\Lambda/k_B T_e$ distributions are shown. Both the dust charge and the electric field decrease with increasing α_0. The decrease of $|Z_d|$ is due to the increase of the number of the positive ions deposited on the dust grain at fixed n_{e0}. Since $eE=-(k_B T_e/n_e)d_x n_e$, the decrease of the electric field can be attributed to the decrease of $d_x n_e$ (see also Fig. 2).

The effect of the neutral-gas pressure p_0 on the forces acting on the dust grain is also studied. The spatial profiles of F_{dr+}, F_{dr-}, and $|Z_d eE|$ for p_0= 100, 200, and 300 mTorr are shown in Fig. 4. One can see from the figure that the positive- and negative-ion drag forces decrease slightly with increasing p_0. This decrease can be attributed to the decrease of the electron temperature, as T_e= 1.78, 1.61, and 1.52 eV for p_0= 100, 200, and 300 mTorr, respectively. The electric field near the discharge boundary increases with increasing p_0 due to the increase of the electron density gradient (see Fig. 5). As a result, at 100 mTorr the total ion drag force $F_{dr+}+F_{dr-}$ is higher than $|Z_d eE|$. However, at $p_0>200$ mTorr the latter becomes dominating.

The forces acting on the dust grain depend also on the grain size. The profiles of F_{dr+}, F_{dr-}, and $|Z_d eE|$ for a_d= 25, 100, and 200 nm are shown in Fig. 6. The forces increase with a_d simply because of the increase of the dust surface that the ions and electrons act on. However, we note that the ratio $|(F_{dr+}+F_{dr-})/Z_d eE|$ decreases with increasing a_d for the parameters considered.

Finally, we compare F_{dr+} and F_{dr-} with the simplified expressions F_{dr+}^{approx} and F_{dr-}^{approx} given by Eqs. (12) and (13), respectively. The profiles of F_{dr+}/F_{dr+}^{approx} and F_{dr-}/F_{dr-}^{approx} for different α_0 are shown in Figs. 7(a) and 7(b), respectively. For completeness, the positive- and negative-ion velocities for $\alpha_0=1$ are given in Fig. 7(c). One can see from the figures that the difference in F_{dr-} and F_{dr-}^{approx} is about the same as that in F_{dr+} and F_{dr+}^{approx}. The maximum deviation F_{dr-} from F_{dr-}^{approx} is about 20%. Thus, the simplified expression (13) may be used for the negative-ion drag force calculation instead of the more complicated (10). The ratio F_{dr-}^{c}/F_{dr-}^{o} is much smaller than F_{dr+}^{c}/F_{dr+}^{o}. At the parameters corresponding to Fig. 7 the ratios F_{dr+}^{c}/F_{dr+}^{o} and F_{dr-}^{c}/F_{dr-}^{o} are about 10^{-2} and 10^{-32}, respectively. The negative-ion-collection force is so small because most of the negative ions in the Maxwellian distribution (8) do not arrive at the dust, and for these ions we have $b_{coll}=0$. Clearly, this is not the case for the positive ions.

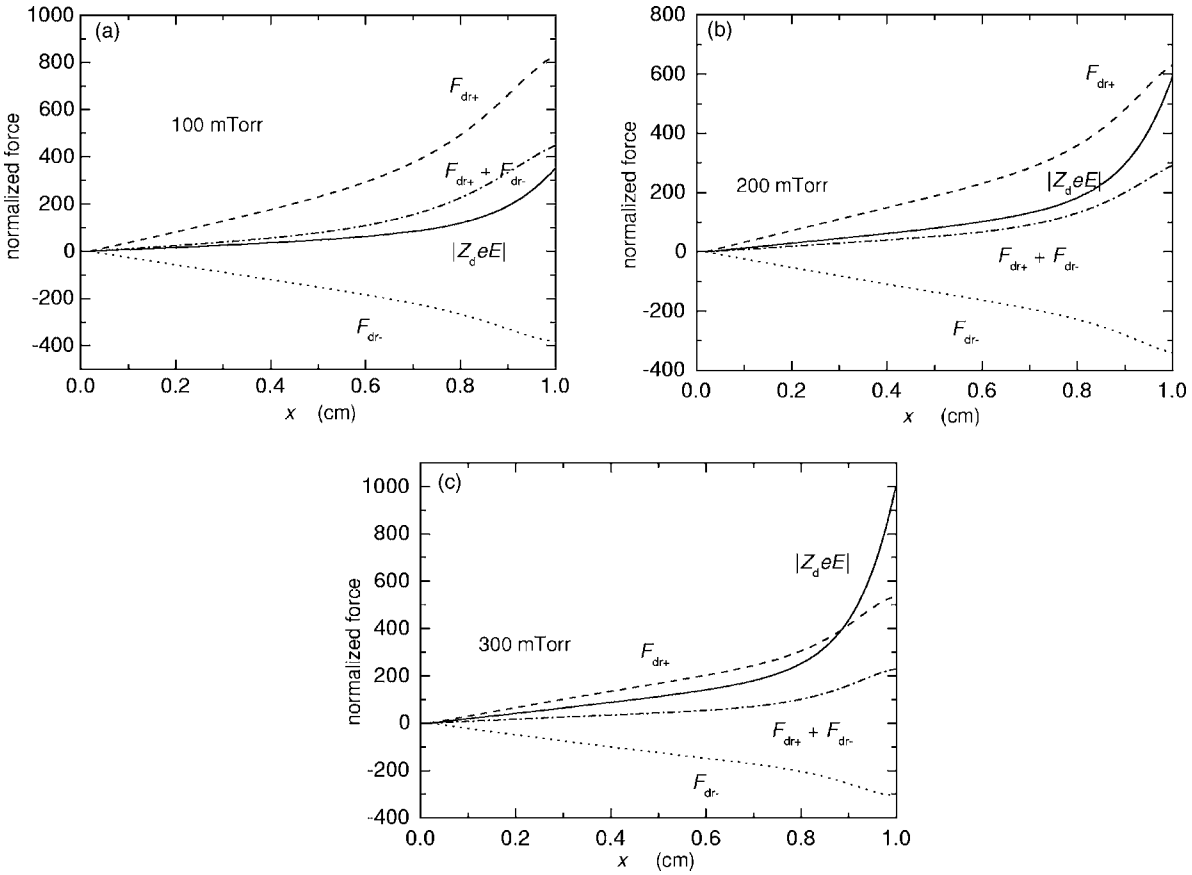

FIG. 4. The normalized forces for different pressures $p_0=100$ (a), 200 (b), and 300 (c) mTorr at $\alpha_0=3$. The other plasma parameters are the same as in Fig. 1.

IV. DISCUSSION

We now discuss the validity of the several simplifications made in our model of the electronegative plasma. First, it is assumed that the electron temperature is spatially uniform throughout the plasma slab. This is a good approximation for the relatively thin slab and not too high neutral-gas pressures considered here. Extensions of the present study to large plasma volumes requires a knowledge of the details of forming and sustaining the plasma by the external energy source, since the mechanism of energy transfer to the plasma electrons and ions in the complex plasma system can affect the parameters involved in an interactive manner [14].

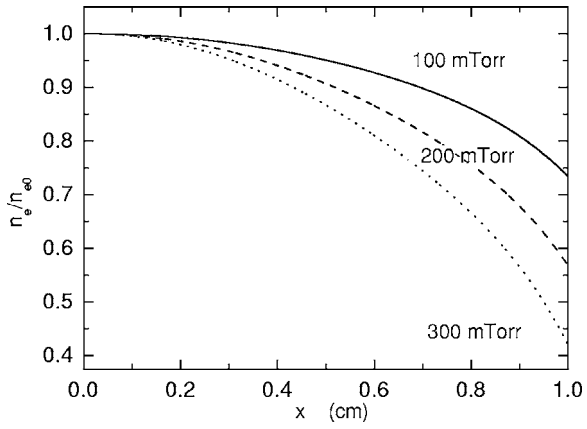

FIG. 5. The normalized electron densities for $p_0=100$, 200, and 300 mTorr. The other plasma parameters are the same as in Fig. 4.

Another simplification is the use of the Debye-Hückel (screened Coulomb) potential [1] in obtaining the orbital momentum-transfer cross sections (11). The Debye-Hückel theory is widely used for objects of small radius compared to the Debye length, such as dust particles. It has been shown that for small ($a_d \sim 10^{-3}\lambda_D$) dust grains the theory gives almost the same potential distribution around the dust as that of the full orbital motion theory [28]. Kilgore *et al.* [29] performed numerical calculations of the positive-ion-dust orbit momentum-transfer cross section for a screened Coulomb potential and for the potential distribution obtained by solving numerically the Poisson-Vlasov system. They found that the differences in the corresponding cross sections are less than 30%. One can expect that the difference in the cross section for the negative-ion-dust interaction will be similar.

The approximation of screened Coulomb potential is applicable when the scattering parameter $\beta(v)=e^2|Z_d|/m_+v^2\lambda_D$ is smaller than unity [30]. The condition $\beta(v)<1$ is justified for the parameters considered here since submicrometer dust grains are considered. In fact, for the conditions of Fig. 1, $\beta(v_{av})$ varies in the range 0.04–0.2, where $v_{av}=\sqrt{8k_BT_+/\pi m_+}$. For micrometer-size dust grains other scattering or interaction mechanisms have to be included. For example, Khrapak *et al.* [30,31] and Ivlev *et al.* [32] have

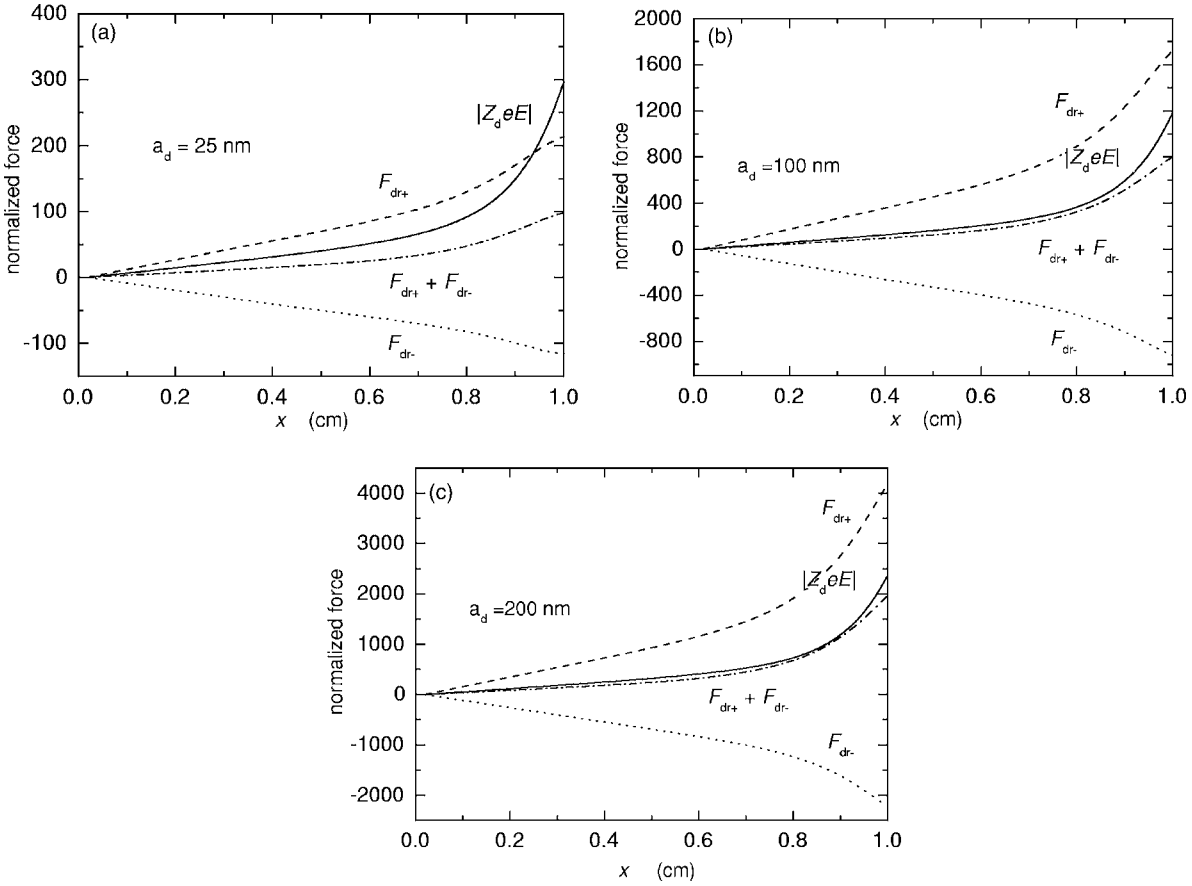

FIG. 6. The normalized forces for different dust radii a_d=25 (a), 100 (b), and 200 (c) nm at $n_{e0}=10^{10}$ cm^{-3}, $\alpha_0=3$, and p_0 =200 mTorr.

proposed theories to calculate the ion drag force for $\beta(v)>1$.

Since we have considered the forces on an isolated dust grain, dust-dust interaction, which can affect the electron and ion grain currents, has been precluded. For example, Tsytovich [33] showed that blocking of the latter currents by neighboring grains can lead to an effective attractive force among the dust grains. Such effects can be important if the dust density is high.

Note that in plasmas with high dust densities the electron density is usually much smaller than the positive-ion density [1]. This case is similar to the case of large α_0 when the ratio n_i/n_e is also large (see Figs. 1–3). We can expect that in plasmas with high dust densities the dust charge and the ion drag and electric forces will be small, as at large α_0. In this case the neutral drag and thermophoresis forces can be important [13].

V. CONCLUSION

The positive- and negative-ion drag and electric forces affecting an isolated submicrometer dust grain in an electronegative plasma have been studied. The study is carried out for the case when the negative ions do not obey the Boltzmann distribution. It is shown that the direction of the negative-ion drag force depends on the negative-ion density n_-. At small n_- the force is directed toward the plasma boundary, and at large negative-ion density the direction is reversed. The directions of the electric and positive-ion drag forces do not depend on n_-. On the other hand, for a negatively charged dust grain the electric and positive-ion drag forces on it are always directed toward and away from the discharge center, respectively.

At high negative-ion densities, the negative-ion drag force is important. The magnitude of the force is near that of the positive ions if the negative- and positive-ion fluxes are of similar magnitude. Due to the negative-ion drag force the total ion drag force acting on an isolated dust grain in an electronegative plasma usually decreases because F_{dr-} is directed toward the discharge center at relatively large negative-ion densities. As a result, at large n_- the total ion drag force can be smaller than the electric force in the entire plasma volume. At small n_- the total ion drag force dominates over $|Z_d eE|$ in the central part of the discharge.

Our study shows that the ratio $|(F_{dr+}+F_{dr-})/Z_d eE|$ strongly depends on the negative-ion density, neutral-gas pressure, and dust size. In particular, by varying the latter parameters one can control the total force $\mathbf{F}_{tot}=\mathbf{F}_{dr+}+\mathbf{F}_{dr-}+Z_d e\mathbf{E}$ acting on a dust grain, in both magnitude and direction.

If the condition $|(F_{dr+}+F_{dr-})/Z_d eE|>1$ is satisfied at the center of the discharge, the dust grains will be driven away from the center and a region void of dusts can appear [11].

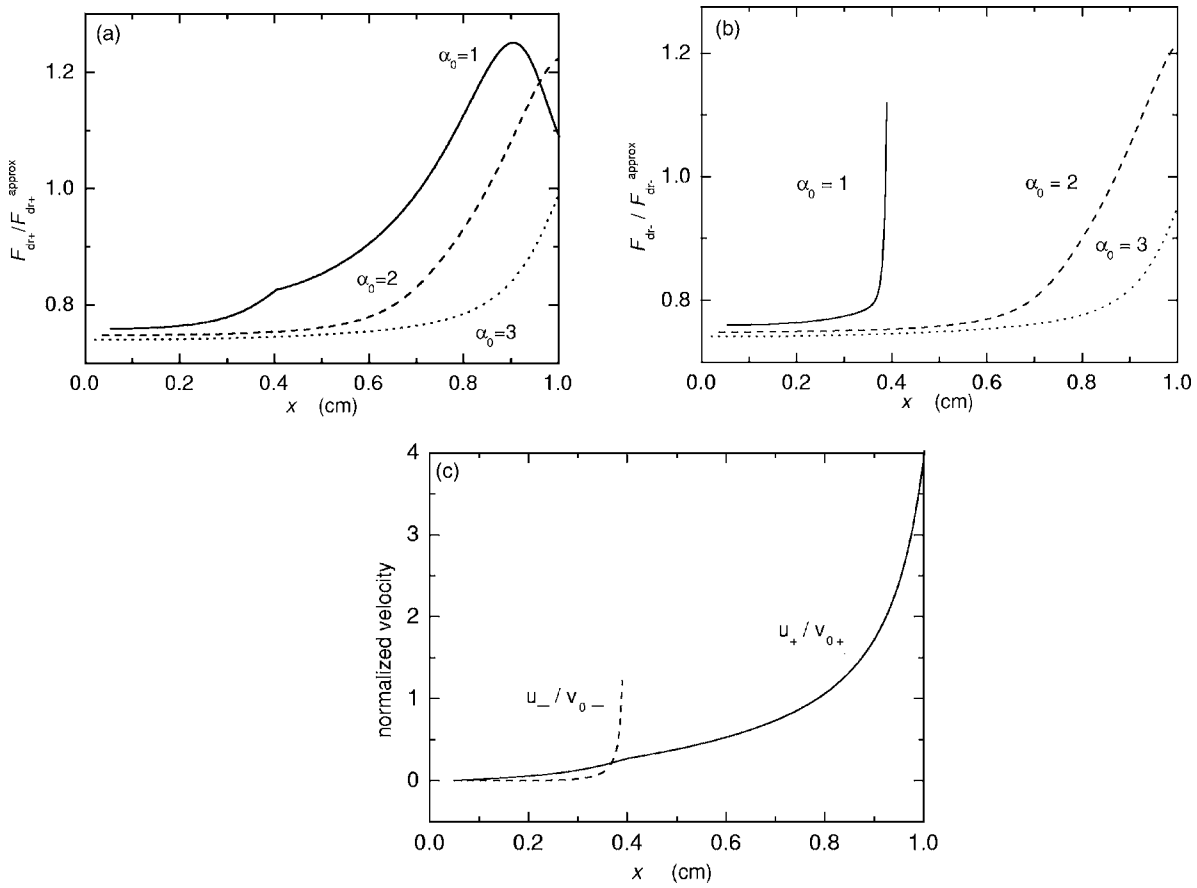

FIG. 7. F_{dr+}/F_{dr+}^{approx} (a) and F_{dr-}/F_{dr-}^{approx} (b) for different negative-ion densities, and the normalized ion velocity profiles (c) for α_0=1. The other plasma parameters are the same as in Fig. 1.

On the other hand, if the inequality is reversed, the total force will be directed toward the center, and one can expect that the grains will be trapped at the center of the plasma, and a ball-like dust cluster will be formed there [8]. In a recent experiment, Arp *et al.* [6] obtained a dust ball by creating an effective center-directed thermophoresis force. Our study here shows that even without the latter force, at sufficiently high negative-ion densities the total force on a dust grain will be directed toward the center of the plasma volume. Thus, dust balls can be created in electronegative complex plasmas by simply increasing the negative-ion density. Such a configuration is clearly useful for more efficient plasma processing of novel functional grains [34] as well as for modeling atomic crystal formation.

ACKNOWLEDGMENTS

One of the authors (I.D.) was supported by the Humboldt Foundation. This work was also supported by A*STAR (Singapore) and AcRF (NTU, Singapore).

[1] *Dusty Plasmas: Physics, Chemistry, and Technological Impacts in Plasma Processing*, edited by A. Bouchoule (Wiley, New York, 1999), and the references therein.
[2] G. E. Morfill, H. M. Thomas, U. Konopka, H. Rothermel, M. Zuzic, A. Ivlev, and J. Goree, Phys. Rev. Lett. **83**, 1598 (1999).
[3] P. K. Shukla and A. A. Mamun, *Introduction to Dusty Plasma Systems* (Institute of Physics, Bristol, 2002).
[4] See, for example, S. V. Vladimirov and K. Ostrikov, Phys. Rep. **393**, 175 (2004).
[5] S. I. Popel, A. P. Golub, T. V. Losseva, A. V. Ivlev, S. A. Khrapak, and G. Morfill, Phys. Rev. E **67**, 056402 (2003).
[6] O. Arp, D. Block, A. Piel, and A. Melzer, Phys. Rev. Lett. **93**, 165004 (2004).
[7] M. Klindworth, A. Piel, A. Melzer, U. Konopka, H. Rothermel, K. Tarantik, and G. E. Morfill, Phys. Rev. Lett. **93**, 195002 (2004).
[8] Z. Chen, M. Y. Yu, and H. Luo, Phys. Scr. **71**, 638 (2005).
[9] G. E. Morfill, H. M. Thomas, U. Konopka, H. Rothermel, M. Zuzic, A. Ivlev, and J. Goree, Phys. Rev. Lett. **83**, 1598 (1999).
[10] M. Mikikian and L. Boufendi, Phys. Plasmas **11**, 3733 (2004).
[11] V. N. Tsytovich, S. V. Vladimirov, and G. E. Morfill, Phys. Rev. E **70**, 066408 (2004), and the references therein.

[12] M. S. Barnes, J. H. Keller, J. C. Forster, J. A. O'Neill, and D. K. Coultas, Phys. Rev. Lett. **68**, 313 (1992).
[13] J. Perrin, P. Molinas-Mata, and P. Belenguer, J. Phys. D **27**, 2499 (1994).
[14] M. A. Lieberman and A. J. Lichtenberg, *Principles of Plasma Discharges and Materials Processing* (Wiley, New York, 1994).
[15] S. V. Vladimirov, K. N. Ostrikov, M. Y. Yu, and G. E. Morfill, Phys. Rev. E **67**, 036406 (2003).
[16] K. Ostrikov, I. B. Denysenko, S. V. Vladimirov, S. Xu, H. Sugai, and M. Y. Yu, Phys. Rev. E **67**, 056408 (2003).
[17] I. B. Denysenko, K. Ostrikov, S. Xu, M. Y. Yu, and C. H. Diong, J. Appl. Phys. **94**, 6097 (2003).
[18] Z. X. Wang, X. Wang, J. Y. Liu, and Y. Liu, J. Appl. Phys. **97**, 023302 (2005).
[19] Z. X. Wang, J. Y. Liu, Y. Liu, and X. Wang, Phys. Plasmas **12**, 012104 (2005).
[20] I. B. Denysenko, M. Y. Yu, L. Stenflo, and N. A. Azarenkov, Phys. Plasmas **12**, 042102 (2005).
[21] E. W. McDaniel and E. A. Mason, *The Mobility and Diffusion of Ions in Gases* (Wiley, New York, 1973).
[22] W. H. Press, B. P. Flannery, S. A. Teukolsky, and W. T. Vetterling, *Numerical Recipes: The Art of Scientific Computing*, (Cambridge University Press, Cambridge, U.K., 1998), p. 572.
[23] J. E. Daugherty and D. B. Graves, J. Appl. Phys. **78**, 2279 (1995).
[24] J. E. Daugherty, R. K. Porteous, M. D. Kilgore, and D. B. Graves, J. Appl. Phys. **72**, 3934 (1992).
[25] S. A. Khrapak and G. E. Morfill, Phys. Rev. E **69**, 066411 (2004).
[26] A. A. Mamun and P. K. Shukla, Phys. Plasmas **10**, 1518 (2003).
[27] M. Yan and W. J. Goedheer, Plasma Sources Sci. Technol. **8**, 349 (1999).
[28] R. V. Kennedy and J. E. Allen, J. Plasma Phys. **69**, 485 (2003).
[29] M. D. Kilgore, J. E. Daugherty, R. K. Porteous, and D. B. Graves, J. Appl. Phys. **73**, 7195 (1993).
[30] S. A. Khrapak, A. V. Ivlev, G. E. Morfill, and H. M. Thomas, Phys. Rev. E **66**, 046414 (2002).
[31] S. A. Khrapak, A. V. Ivlev, G. E. Morfill, and S. K. Zhdanov, Phys. Rev. Lett. **90**, 225002 (2003).
[32] A. V. Ivlev, S. A. Khrapak, S. K. Zhdanov, G. E. Morfill, and G. Joyce, Phys. Rev. Lett. **92**, 205007 (2004).
[33] V. N. Tsytovich and G. E. Morfill, Plasma Phys. Controlled Fusion **46**, B527 (2004).
[34] M. J. Pitkethly, Mater. Today **6**(12), Suppl. 1, 36 (2003).